

1 **Global-scale shifts in Anthropocene rooting depths pose unexamined consequences**
2 **for critical zone functioning**

3 Emma Hauser¹, Pamela L. Sullivan², Alejandro N. Flores³, Daniel Hirmas⁴, Sharon A. Billings¹

4 ¹Department of Ecology and Evolutionary Biology and Kansas Biological Survey and Center for
5 Ecological Research, The University of Kansas, Lawrence, KS, USA.

6 ²College of Earth, Ocean, and Atmospheric Science, Oregon State University, Corvallis, OR,
7 USA.

8 ³Department of Geosciences, Boise State University, Boise, ID, USA

9 ⁴ Department of Environmental Sciences, University of California, Riverside, CA, USA.

10 Corresponding author: Emma Hauser, Sharon Billings (emma.hauser@umt.edu,
11 sharon.billings@ku.edu)

12
13 **Key Points:**

- 14 • Rooting depths are changing globally; the depth to which 99% of crop roots extend is
15 shallower by ~ 60 cm compared to natural systems.
- 16 • In other regions, such as those experiencing woody encroachment, roots are deepening by
17 ~38 cm compared to previous dominant vegetation.
- 18 • These opposing phenomena result in average rooting depths that are ~8 cm shallower
19 today and projected to become ~30 cm shallower by 2100.
- 20

21 Abstract

22 Rooting depth is an ecosystem trait that determines the extent of soil development and carbon
23 (C) and water cycling. Recent hypotheses propose that human-induced changes to Earth's
24 biogeochemical cycles propagate deeply due to rooting depth changes from agricultural and
25 climate-induced land cover changes. Yet, the lack of a global-scale quantification of rooting
26 depth responses to human activity limits knowledge of hydrosphere-atmosphere-lithosphere
27 feedbacks in the Anthropocene. Here we use land cover datasets to demonstrate that root depth
28 distributions are changing globally as a consequence of agricultural expansion truncating depths
29 above which 99% of root biomass occurs (D99) by ~60 cm, and woody encroachment linked to
30 anthropogenic climate change extending D99 in other regions by ~38 cm. The net result of these
31 two opposing drivers is a global reduction of D99 by 5%, or ~8 cm, representing a loss of
32 ~11,600 km³ of rooted volume. Projected land cover scenarios in 2100 suggest additional future
33 D99 shallowing of up to 30 cm, generating further losses of rooted volume of ~43,500 km³,
34 values exceeding root losses experienced to date and suggesting that the pace of root shallowing
35 will quicken in the coming century. Losses of Earth's deepest roots — soil-forming agents —
36 suggest unanticipated changes in fluxes of water, solutes, and C. Two important messages
37 emerge from our analyses: dynamic, human-modified root distributions should be incorporated
38 into earth systems models, and a significant gap in deep root research inhibits accurate
39 projections of future root distributions and their biogeochemical consequences.

40 Plain Language Summary

41 The distribution of plant roots helps determine the extent of nutrient, C and water cycling
42 beneath Earth's surface. Human activities, including land use and climate change, can change the
43 distribution of plant roots and their activities across the globe. Here, we used global land cover
44 datasets in combination with field-generated rooting depth equations to estimate global scale
45 changes to roots both now and into the future. Globally, roots are shallower than they would be
46 in the absence of human activity due to extensive land conversion to agriculture. In some
47 regions, human-promoted woody encroachment induces root elongation, but this effect is
48 overwhelmed by the spatial extent of agricultural conversion. In the future, roots likely will
49 become shallower at an even faster pace. In future projections, deep roots appear especially
50 vulnerable to loss, prompting numerous questions for additional field- and modeling-based

51 studies about the ways nutrients, C, and water will cycle in a future with fewer deep roots. We
52 provide a foundation for those questions by demonstrating human influence on the roots that
53 shape the character of Earth's skin.

54 **1 Introduction**

55 Roots are subsurface engineers, and their distributions drive ecosystem-scale processes (Maeght
56 et al., 2013; Pierret et al., 2016; Sullivan et al., 2022) such as soil development (Brantley et al.,
57 2017; Hasenmueller et al., 2017; Austin et al., 2018), release of mineral-bound nutrients
58 (Jobbagy & Jackson, 2001; Hasenmueller et al., 2017; Austin et al., 2018), subsoil water flow
59 paths and residence time (Zhang et al., 2015; Fan et al., 2017) , and deep C fluxes (Richter and
60 Markewitz, 1995; Schenk, 2007; Pierret et al., 2016; Fan et al., 2017; Billings et al., 2018). The
61 dominant drivers of rooting distributions are plant functional type (PFT, Jackson et al., 1996) and
62 variation in water availability (Schenk, 2007; Nippert et al., 2007; Fan et al., 2017), both of
63 which are changing in response to anthropogenic land cover conversion, as well as altered
64 atmospheric composition and concomitant changes in climate (Edgeworth et al., 2001; Cramer et
65 al., 2010; Ellis et al., 2010). This observation suggests that rooting depth distributions are likely
66 undergoing changes due to human activities in the critical zone (CZ, Earth's living skin, Jordan
67 et al., 2001).

68
69 Quantifying large-scale, human-induced changes to rooting distributions and how they may
70 differ regionally is a critical step towards a greater understanding of how roots govern large-
71 scale, sub-surface and surface processes. In spite of widespread recognition of the importance of
72 root depth (Maeght et al., 2013; Pierret et al., 2016) and a growing recognition of the great
73 depths to which roots can penetrate (Stone & Kalisz, 1991; Nepstad et al., 1994; Canadell et al.,
74 1996; Schenk & Jackson, 2002a; Schenk & Jackson et al., 2002b; Fan et al., 2017), large-scale
75 responses of rooting depths to anthropogenic perturbations of the biosphere have been poorly
76 characterized. This knowledge gap is due in part to the challenges of accessing relatively deep
77 soil horizons (Maeght et al., 2013), as well as the challenge of unraveling the vast complexity of
78 Earth's subsurface systems. One consequence of poorly defined rooting distributions at large
79 spatial scales is generalized representations of rooting parameters in land models (McCormack et
80 al., 2015; Iversen et al., 2017; McCormack et al., 2017). Although many land models, such as the
81 Community Land Model (CLM), represent changes to roots with land use change (Lawrence et

82 al., 2019), some land cover types are not well represented in these models. For example, crops in
83 CLMs are assigned the same rooting depth as C3 grasses (Lawrence et al., 2019), though row
84 crops, in particular, typically have far shallower roots than perennial plants (Canadell et al.,
85 1996; DuPont et al., 2014; Billings et al., 2018). Given the plethora of CZ functions influenced
86 by roots (Maeght et al., 2013; Pierret et al., 2016), poor characterization of rooting depths likely
87 limits the accuracy of projected responses of the coupled terrestrial water, energy, and C cycles
88 to climate in the Anthropocene.

89
90 Two Anthropocene phenomena occur at sufficient magnitude to potentially alter rooting
91 distributions at the global scale. First, many regions have experienced conversion to annual row
92 crops (Ramankutty & Foley, 1999; Ellis et al., 2010), a process that induces mortality of deep
93 perennial root systems and replaces them with relatively shallow roots (Billings et al., 2018). In
94 contrast, climate change and increasing atmospheric CO₂ concentrations are linked to root
95 extension of extant woody plants (Iversen, 2010), and shifting ecoregion ranges may increase
96 rooting depths where more deeply rooted woody vegetation becomes increasingly abundant in
97 grasslands and tundra (Jackson et al., 1996; Harsch et al., 2009; Stevens et al., 2017; Wang et al.,
98 2019). Studies exploring rooting depth typically focus on absolute rooting depths and their
99 responses to climate or atmospheric CO₂ (Kleidon & Heimann, 1998; Kleidon, 2003) or,
100 separately, land cover changes in specific regions of interest (Jaramillo et al., 2003; Hertel et al.,
101 2009; DuPont et al., 2010). Despite known changes in global land cover (Ellis et al., 2010) that
102 are associated with distinct rooting depths (Jackson et al., 1996; Zeng, 2001), as well as global
103 analyses of the maximum extent of contemporary root depths (Schenk & Jackson, 2002a; Schenk
104 & Jackson, 2002b; Schenk & Jackson, 2005), to date, no one has directly quantified the net
105 change in rooting distributions at the global scale as a consequence of these opposing human
106 activities.

107
108 Here we provide a first estimate of the extent to which rooting depths increase or decrease in
109 response to land use and climate change and the volume of soil affected by this change. We also
110 project how rooting depths and rooted volumes may change throughout the 21st century as more
111 land is converted to agricultural and urban use, and as biome ranges continue to shift with
112 changing climate. We emphasize that our focus is not on maximum rooting depths. Indeed, there

113 is a growing appreciation of the great depths to which vegetation can root (Stone & Kalisz 1991;
114 Schenk & Jackson, 2002a; Schenk & Jackson, 2005; Maeght et al., 2013; Pierret et al., 2016; Fan
115 et al., 2017) though the true maximum rooting depth may never be known in some systems
116 (Kleidon, 2003; Pierret et al., 2016; Fan et al., 2017). Instead, we focus on the depths to which
117 most or half (i.e., 99%, 95%, and 50%) of the root biomass of an ecosystem extends (Zeng,
118 2001), as well as changes to rooted soil volume. These metrics highlight the depths within which
119 most roots reside as well as the soil volume through which most root distribution changes occur,
120 both functionally consequential measures. Additionally, these metrics represent those for which
121 much data exist, enabling the cross-system comparisons necessary to estimate the spatial extent
122 of rooting depth changes in the Anthropocene. Our work thus reveals how anthropogenic, global-
123 scale changes in rooting depth metrics are changing, thereby illuminating critical next steps to
124 help us understand future CZ functioning.

125 **2 Materials and Methods**

126 We estimated the volume of soil influenced by human-promoted modification of root
127 distributions. To do this, we estimated potential (i.e., no human influence), contemporary, and
128 projected root distributions at the global scale by combining biome-specific rooting depth
129 functions derived from empirical studies (described below) with spatially explicit land cover
130 datasets. As a part of this process, we examined multiple datasets that, in theory, could help us
131 estimate how humans modify rooting distributions. First, we offer a description of selected
132 datasets followed by an explanation of our selection from those available.

133

134 We used satellite-derived, potential vegetation representing 15 land cover classes (Haxeltine &
135 Prentice, 1996) and their potential global distribution in the absence of human activity at a 5-
136 minute spatial resolution (Ramankutty & Foley, 1999). We compared potential vegetation
137 classes to contemporary land cover as defined by the Global Land Cover 2000 (GLC2000)
138 dataset (Bartolome & Belward, 2005). GLC2000 represents 22 land cover types, which are
139 designated according to plant functional types ascribed to satellite images and ground-truthed by
140 regional analysts. We aligned contemporary vegetation classifications with potential vegetation
141 classes according to previously published frameworks for ecoregion designation (Bartolome &
142 Belward, 2005), and augmented these classes to include a class for permafrost regions where

143 rooting depth is likely limited (Billings et al., 1997; Boike et al., 2018). These efforts resulted in
144 25 distinct land cover types for which rooting depths were assigned. Projected vegetation classes
145 were similarly developed for four Shared Socioeconomic Pathway (SSP) and Representative
146 Concentrations Pathway (RCP) scenarios using spatial projections of gridded, $0.5^\circ \times 0.5^\circ$
147 resolution land covers for the year 2100 (Hurt et al., 2011). All maps were adjusted to the same
148 resolution for analyses using the Raster package in R (Hijmans et al., 2019).

149
150 For all vegetation datasets except those above 60°N (described below), we estimated biome-
151 specific rooting depths by assigning rooting depth functions derived from empirical data
152 compiled in the Fine Root Ecology Database (FRED) and the National Ecological Observatory
153 Network (NEON) database (Iversen et al., 2021; NEON 2021). These datasets have recently
154 expanded rooting depth knowledge beyond earlier works (e.g., Jackson et al., 1996; Zeng, 2001;
155 Schenk and Jackson, 2005) by accumulating new datapoints detailing root trait and distribution
156 patterns in diverse biomes (Krasowski et al., 2018; Montagnoli et al., 2018; Lozanova et al.,
157 2019; Andrade et al., 2020). However, to date no one has harmonized and analyzed these
158 datasets to produce equations describing global rooting depth distributions. Their use here thus
159 represents an advance in the ways we represent rooting depths and their distributions across the
160 globe. Specifically, we used these datasets to estimate the depths by which rooting systems
161 exhibit 50% (D50), 95% (D95), and 99% (D99) of their total biomass in each land cover type. To
162 generate rooting depth functions, we assigned FRED and NEON rooting depth data to biomes
163 according to the position of each datapoint on our modified GLC2000 land cover map. Each set
164 of points was checked using Google Earth to ensure that datapoints were correctly assigned. Due
165 to the resolution of the GLC2000 map, some shrubland and woodland categories were
166 incorrectly identified as cropland; for these points, we reassigned shrub-covered areas to the
167 open-closed deciduous shrubland class and woodlands to the open broadleaved deciduous forest
168 class. We then fit depth-decay curves to each set of points for each biome using the model
169 presented by Zeng (2001). Parameter values and their confidence intervals were obtained for
170 depth-decay curves using a bootstrap procedure where curves were fit to randomly-selected
171 samples (with replacement) of each set of points 1200 times as recommended by Lander (2013).
172 By using the Zeng (2001) model, we assumed that rooting depth distributions remain similar for
173 each vegetation functional type in the potential, contemporary, and future scenarios. The merit of

174 this assumption may vary with time but keeping the rooting depth of each biome's vegetation
175 type consistent across the Holocene and into the future allows us to parse the influence of land
176 cover change on rooting depths from that of less well-characterized phenomena.

177

178 To match the land cover classifications used in potential and contemporary vegetation maps to
179 biome classifications for which we have rooting depth equations, we modified estimated rooting
180 depth distributions for several land covers based on findings from region-specific literature. For
181 example, potential land cover datasets combine both polar and mid-latitude deserts into a single
182 desert category based on hydrologic regimes, yet rooting depths in polar deserts are often
183 constrained by permafrost. We thus separated these two desert regions, reassigning deserts in
184 polar regions to the 'tundra' classification above 60°N (Zhang et al., 2008). Further, in potential
185 and contemporary vegetation datasets, we reassigned evergreen forest and mixed vegetation
186 classes above 50°N to the 'boreal' vegetation classification given previously generated
187 vegetation maps of northern region forests (Brandt et al., 2013; Price et al., 2013), and also
188 assigned herbaceous and shrubland classes above 60°N to the class 'tundra' because these
189 regions exhibit low stature vegetation and lie in previously described tundra areas (Zhang et al.,
190 2008). To generate maps of rooting depth, we gave potential vegetation above 60°N that was
191 previously assigned to the polar desert class a rooting depth specific to permafrost-underlain
192 regions, where roots typically do not penetrate deeper than 30 cm and 50% of root biomass is
193 typically found within 10 cm (Billings et al., 1997; Zhang et al., 2008; Boike et al., 2018; Keuper
194 et al. 2020). For contemporary rooting depth maps, regions above 60°N were all assigned to
195 either a permafrost underlain tundra class or boreal class, which reflect recent measurements in
196 FRED and NEON datasets. Finally, because many remote sensing-based studies of regional
197 ecosystem fluxes omit large, lower latitude desert regions from their analyses due to the lack of
198 quantifiable ecosystem productivity in these systems (Zhao et al., 2005b), we omitted mid-
199 latitude deserts from rooting depth averages reported in the main text. Instead, we present rooting
200 depth metrics that incorporate the potential contribution of these mid-latitude deserts to global
201 root averages in Table 1 of the Supporting Information. Comparison of these results with those
202 reported in the text reveal an inflated influence of mid-latitude desert rooting depth estimates on
203 global averages that likely does not represent reality due to the low density of plants in true
204 deserts (Whitford & Duval, 2019). Ice-covered regions were also omitted from the analyses.

205

206 To assess potential effects of global-scale perturbations projected by the year 2100 on rooting
207 depth distributions, we examined multiple SSP and RCP land cover projections from the
208 Intergovernmental Panel on Climate Change (IPCC). Projected vegetation classes were
209 developed for 4 SSP RCP scenarios (SSP2 RCP4.5, SSP1 RCP2.6, SSP4 RCP6.0, SSP5
210 RCP8.5). Landuse Harmonization datasets designate land cover classes more coarsely than either
211 GLC2000 or potential vegetation datasets, delineating primary and secondary forest regions,
212 primary and secondary non-forest regions, five agricultural classes, pastureland, rangeland, and
213 urban regions (Hurtt et al., 2011). We assigned a rooting depth equation derived from
214 agricultural croplands in the FRED and NEON datasets to all five agricultural classes in the
215 Landuse Harmonization dataset. For secondary non-forests, pastures, and rangelands we
216 assigned rooting depth equations representing herbaceous and grassland systems in the FRED
217 and NEON datasets. Because most secondary forests in these scenarios were in the boreal region,
218 we assigned secondary forests the average root depth value (107.5 cm) of mixed forests (130 cm)
219 and boreal forests (85 cm). Primary forests were assigned depth values generated from the
220 average of all forest classes in the contemporary dataset, and primary non-forests were assigned
221 depths generated by averaging contemporary grassland and shrubland classes. Reflecting
222 anticipated warming and large projected losses of permafrost in the northern hemisphere
223 (Lawrence & Slater, 2005), rooting depths assigned in all future scenarios removed permafrost
224 constraints.

225

226 We examined multiple datasets describing contemporary global root distributions (Schenk and
227 Jackson, 2009) and landcover scenarios across time (Hurtt et al., 2011) as potential candidates
228 for addressing the degree to which humans modify the rooted volume of Earth's subsurface.
229 Such datasets have been pivotal in developing our understanding of and appreciation for the
230 depths of deep roots (Schenk & Jackson, 2005; Schenk, 2005; Pierret et al., 2016), and the
231 Landuse Harmonization (LUH) scenarios represent the best available data for future land cover
232 classifications to date (Hurtt et al., 2020). However, the Schenk and Jackson dataset does not
233 describe roots in agricultural lands, ploughed and fertilized lands, or wetlands (Schenk and
234 Jackson, 2005), and is not divided into land cover classes that can be integrated with datasets
235 describing potential and future land cover scenarios. The LUH scenarios combine land cover

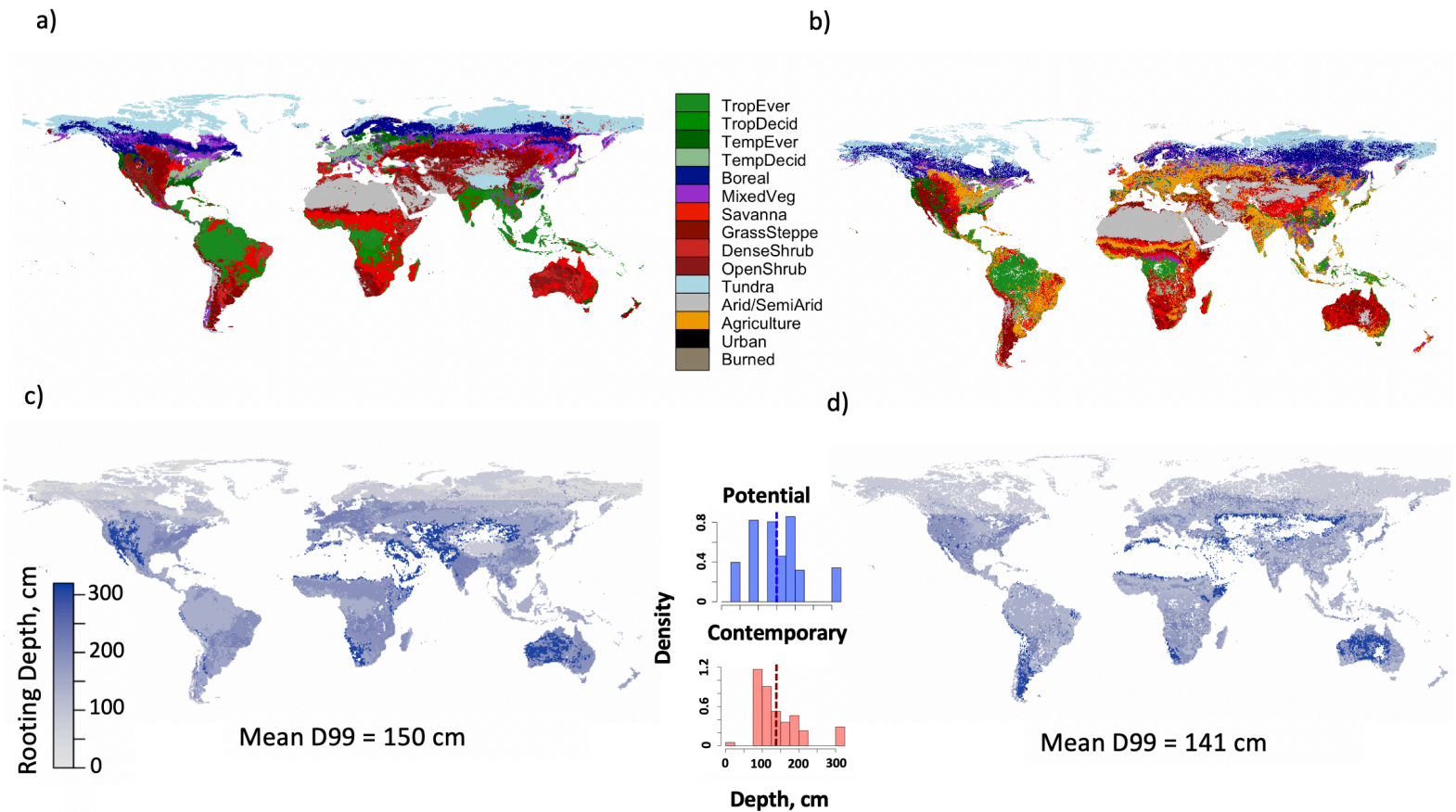
236 classes in ways that result in the loss of important nuances in root distribution estimates in past
237 and contemporary scenarios. For example, all forest types in LUH scenarios are grouped into
238 ‘secondary’ and ‘primary’ forest rather than more region-specific forest classifications (Hurt et
239 al., 2020). In contrast, employing the GLC2000 vegetation classes with rooting depths derived
240 from FRED and NEON data, which include data from Jackson et al. (1996), permitted us to
241 examine two key features of interest. First, this approach permitted incorporation of agricultural
242 land cover classes — a feature that is absent in datasets featuring root distributions alone.
243 Second, the Ramankutty and Foley (1999) dataset serves as the only spatially quantified
244 representation of the potential land cover in the absence of human activity at a 5-minute
245 resolution, allowing for detailed backcasting of estimates of human-induced changes to roots.

246

247 Using the R raster package (RStudio Team, 2017; Hijmans et al., 2019), we assigned rooting
248 depth values to each land cover classification of the potential, contemporary, and projected
249 vegetation maps, and calculated global means of each depth metric. After determining the
250 differences in rooting depths across scenarios, we examined the spatial extent of depth changes
251 to determine differences in rooted volume across scenarios. We then compared metrics across
252 time using 95% confidence intervals of the mean estimates of global rooting depth metrics.
253 Estimates of rooting depth, reflect measurement uncertainty, particularly at deeper depths
254 (Schenk and Jackson, 2002b). However, because we applied root measurements in a consistent
255 manner across potential, contemporary, and projected vegetation maps, we can assess relative
256 differences of root distributions across these different scenarios. We performed correlated t-tests
257 on pairs of rasterized parameter estimate maps (i.e., potential vs. contemporary, and
258 contemporary vs. projected) to determine whether differences between these estimated rooting
259 depth metrics are significantly different from zero. Data were assessed to ensure they met the
260 assumptions of correlated t-tests, including independence of observations, normal distribution of
261 the dependent variable, and no dependent variable outliers. Where data did not meet the
262 assumptions, we ran Wilcoxon tests on the dataset pairs to assess differences in root depth
263 metrics and reported the V-statistics and associated *P*-values generated from those tests.

264 **3 Results**

265 Comparisons of potential and contemporary land cover (Figures 1a and b) and their estimated
 266 rooting depths (Figures 1c and d) suggest that spatially averaged, global values of D99 are the
 267 net result of two competing phenomena: shallowing of roots in agricultural regions and
 268 deepening of roots in regions experiencing woody encroachment. Specifically, the global
 269 average D99 is 5% shallower (8 cm) under contemporary land cover distributions than if
 270 potential vegetation cover types covered Earth's terrestrial surface ($V = 7.11 \times 10^{11}$, Wilcoxon P
 271 < 0.0001 ; Figures 1c and d, Table S1). This represents a loss of rooted volume of $\sim 11,600 \text{ km}^3$.
 272 Values of D95 for contemporary land cover also express similar trends of root shallowing (6% or
 273 5 cm, loss of $\sim 7250 \text{ km}^3$; $V = 7.06 \times 10^{11}$, Wilcoxon $P < 0.0001$; Figures S1a and b). Depth to
 274 50% root biomass (D50), by comparison, displays relatively greater variation between
 275 contemporary and potential land cover, becoming 21% shallower (1.5 cm, 1300 km^3 , $V = 5.32 \times$
 276 10^{11} , Wilcoxon $P < 0.0001$) on average (Figure S2).

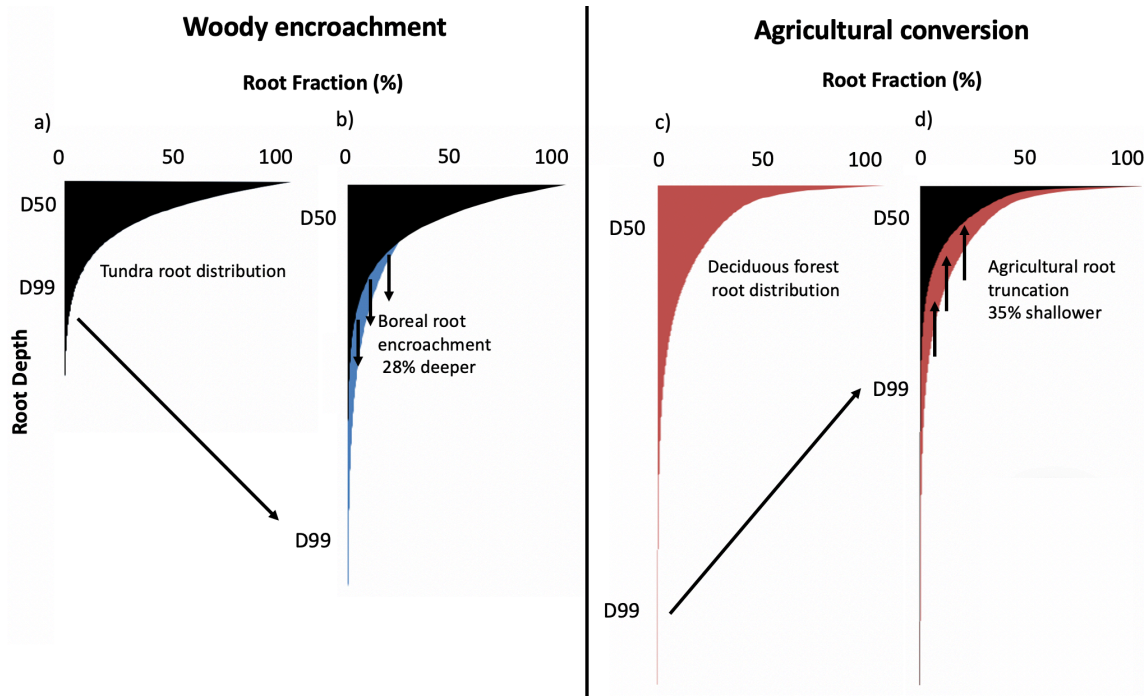


277 **Figure 1.** Land cover and associated rooting depths under potential vegetation in the absence of human influence
 278 (left column) and current vegetation distribution (right column). (a) Potential vegetation cover in the absence of

279 human activity (b) Contemporary land cover distribution from Global Land Cover 2000 (GLC2000), modified to
280 correspond to potential vegetation land cover classifications. (c) and (d) depict depths by which 99% of rooting
281 biomass occurs (D99) under potential (c) and contemporary (d) land cover types. Inset histogram displays rooting
282 depth distributions. Blue histogram reflects potential vegetation data, and red histogram contemporary land cover.
283 Dashed vertical lines represent means. Appearance of a distinct color change from dark blue to light grey in Asia
284 and Canada at 60°N in (c) is an artifact of restricting maximum rooting depth assignments to reflect well-
285 characterized limitations imposed by frozen soils; this distinction is less evident in contemporary D99 maps (d)
286 because of the higher spatial resolution of the GLC2000 dataset. Appearance of a distinct line at 50°N, especially
287 evident in (d), reflects reassignment of mixed forests to the boreal forest class above this latitude (Brandt et al.,
288 2013; Price et al., 2013). See text for reassignment details. While these lines are unrealistic, it reflects our current
289 knowledge about root depths in northern regions and demonstrates the remaining need for additional work
290 combining cryospheric studies and soil science to characterize root systems at relatively high latitudes.

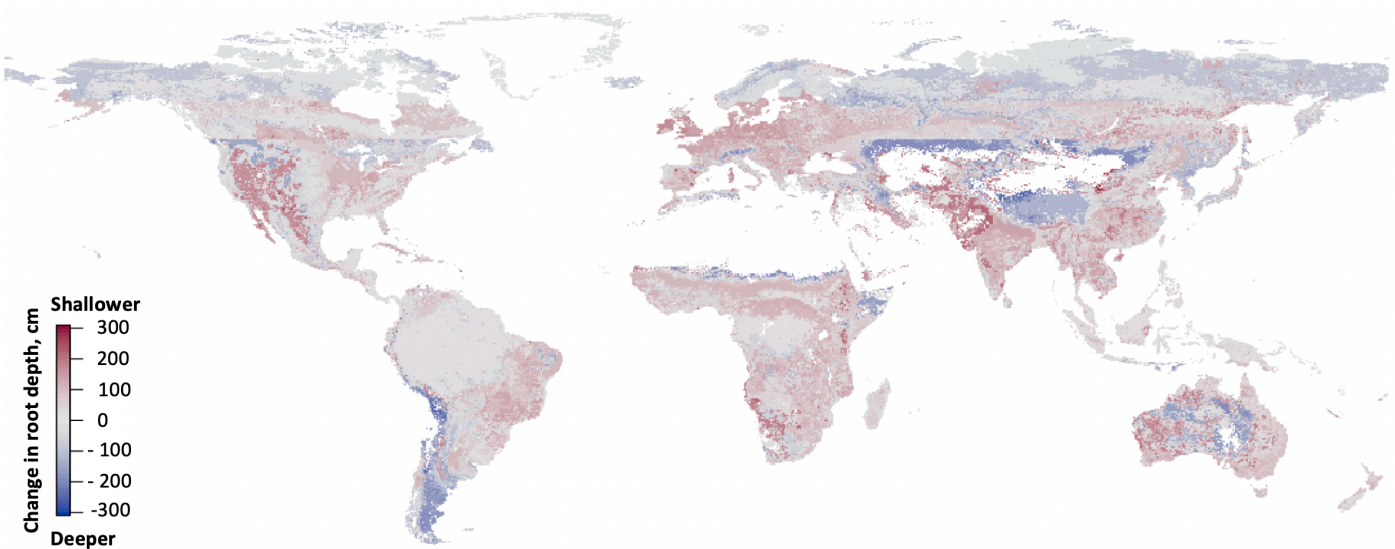
291
292 Agricultural land conversion serves as a dominant influence on these global trends (Figures 2
293 and 3). Regions where roots experienced shallowing during the shift from potential to
294 contemporary land cover are on average 43 cm shallower (23%) than potential vegetation
295 distributions and represent ~48% of Earth's land surface (7.01×10^7 ha; Fig. 3). Thirty three
296 percent of shallowing regions (2.28×10^7 ha) experience agricultural expansion. In these areas,
297 perennial vegetation has been converted to agricultural land (defined here as annual crops and
298 managed pasture), such that D99 has decreased by as much as 33% (60 cm). The remaining
299 shallowing occurs primarily in some northern and arid regions, possibly due to increased
300 disturbance (Harsch et al., 2009; Wang et al., 2020, Hurtt et al., 2020), urbanization (Lindsey &
301 Bassuk, 1992; Day et al. 2010) and desertification (Lal, 2001, Zhao et al., 2005b). Where
302 woody encroachment is evident in contemporary land cover data, D99 increased relative to
303 potential vegetation by up to 39% (38 cm; note that here we use the phrase 'woody
304 encroachment' to refer to both shrubland encroachment into grasslands, and forest encroachment
305 into Arctic and alpine tundra). This result may overestimate current rooting depths if the rooting
306 depths we assigned were derived from well-established, mature systems, given that woody plants
307 in recently encroached systems likely have not yet achieved such depths (Stevens et al., 2017;
308 Billings et al., 2018). Despite this possible overestimation, root deepening via woody
309 encroachment does not overcome the effect of root shallowing, in part because of the smaller
310 total fraction of Earth's terrestrial surface experiencing woody encroachment (35% or $5.06 \times$
311 10^7 ha).

312
313



314
315
316
317
318

Figure 2. Representation of rooting depth elongation due to woody encroachment (a and b) and rooting depth truncation due to agricultural expansion (c and d). Blue region in B demonstrates the belowground increase in roots shown in blue in Figure 3. Red region in D exemplifies loss of rooting system depth for red regions in Figure 3.



319
320
321
322

Figure 3. Mapped differences between potential and contemporary rooting depths. Red cells indicate a decrease in the depth to 99% of rooting biomass (D99) while blue cells indicate an increase in D99 resulting from contemporary vegetation distributions. Appearance of a distinct color change from dark blue to light grey and red in Asia and

323 Canada at 50°N reflects reassignment of mixed forests to the boreal forest class above this latitude (Brandt et al.,
 324 2013; Price et al., 2013). See Figure 1 caption for additional explanation.

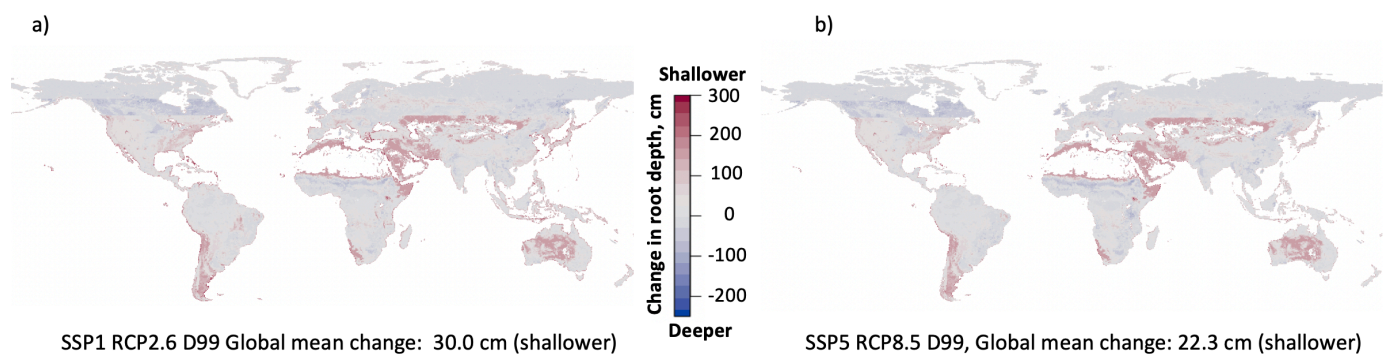
325

326 Changes to rooting distributions by the year 2100 vary under different potential scenarios of
 327 climate and land use change as well as different societal responses to those changes. The SSP
 328 scenarios examined here represent global narratives including a scenario with few roadblocks to
 329 both mitigation of and adaptation to climate change (SSP1), moderate challenges to mitigation
 330 and adaptation (SSP2), a scenario of social inequality with many challenges to adaptation but
 331 few for mitigation (SSP4), and a strategy of fossil fuel dependence with many challenges to
 332 mitigation but few to social adaptation (SSP 5, Riahi et al., 2017). These narratives are used in
 333 conjunction with projected land use and climate (RCP) scenarios to model future societal and
 334 ecological conditions, on which we rely for our rooting distribution estimates.

335

336 Projections for the year 2100 suggest that the scenario with the largest cropland increase and
 337 relatively low radiative forcing enhancement from current levels (SSP1 RCP2.6, Figure 4a)
 338 generates the most extreme reduction of deep roots, truncating values of D99 by 30 cm ($V = 2.16$
 339 $\times 10^{10}$, Wilcoxon $P < 0.0001$). The smallest shallowing of D99, 22.3 cm ($V = 1.77 \times$
 340 10^{10} , Wilcoxon $P < 0.0001$), occurs under the highest emissions scenario (SSP5 RCP8.5, Figure
 341 4b). As a result, the future rooted volume will be reduced by $\sim 32,400 \text{ km}^3$ to $\sim 43,500 \text{ km}^3$.

342



343

344

345 **Figure 4.** Projected changes of depth to 99% rooting biomass (D99) by the year 2100 relative to contemporary
 346 rooting depth distributions. Projections are based on land use and emissions changes under two combinations of
 347 Shared Socioeconomic Pathways (SSP) and Representative Concentration Pathways (RCP), SSP1 RCP2.6 (a) and
 348 SSP5 RCP8.5 (b). These two maps represent the scenario of greatest and least projected change, respectively. Red
 349 colors indicate root depth truncation or shallowing, and blue indicates elongation or deepening. Appearance of a

350 distinct color change from dark red to light grey in Asia at 50°N reflects reassignment of mixed forests to the boreal
351 forest class above this latitude (Brandt et al., 2013; Price et al., 2013; see text for reassignment details).

352

353 Values of D50 for the year 2100 experience a shallowing of 3 cm across all assessed scenarios
354 ($V = 2.47 \times 10^{10}$, Wilcoxon $P < 0.0001$; Figure S5), representing a loss of rooted soil volume of
355 $\sim 4400 \text{ km}^3$. Though small relative to changes in deep root systems, this D50 shallowing is
356 double that occurring during the previous $\sim 10,000 \text{ y}$ (Gupta, 2004) of anthropogenic land
357 conversion (Figure S6).

358 **4 Discussion**

359 Our estimates of rooting depth and rooted soil volume suggest that root biomass throughout
360 Earth's soils, even deep in the subsurface, has been and will continue to be vulnerable to human
361 influence (Figures 2, 3, 4). Although maximum rooting depths are poorly characterized and are
362 likely deeper than is typically appreciated (Maeght et al., 2013; Pierret et al., 2016; Fan et al.,
363 2017), we demonstrate that the depths to which most or half of all rooting biomass reach (i.e.,
364 D99, D95, and D50) currently reflect human-induced, global-scale changes in land cover (Figure
365 1). We further demonstrate that root shallowing in agricultural regions ($\sim 60 \text{ cm}$ across $2.28 \times$
366 10^7 ha for D99) and root deepening in regions experiencing woody encroachment ($\sim 38 \text{ cm}$
367 across $5.06 \times 10^7 \text{ ha}$ for D99) result in a globally-averaged estimate of net 8 cm shallowing of
368 D99 values. This represents a net loss of $\sim 11,600 \text{ km}^3$ of rooted volume to date in the
369 Anthropocene.

370

371 In the future, rooting depth scenarios might be expected to reflect the elongating effects of
372 woody encroachment on D99, D95, D50 and rooted soil volume to a yet greater extent, given the
373 apparent role of rising atmospheric CO_2 concentrations in promoting woody encroachment
374 (Devine et al. 2017). However, the four IPCC scenarios explored here suggest that by 2100,
375 globally-averaged rooting distributions may become yet shallower relative to contemporary
376 rooting depths (Figures 4, S4 and S5). Reduced rooting depths by 2100 are driven by substantial
377 root shallowing across regions of Africa, the Middle East, Asia and Australia (Fig. 4), where
378 deeply rooted shrublands are projected to transition to herbaceous grasslands and where there is
379 continued agricultural and pasture expansion (Hurtt et al. 2020). In both cases, a more shallowly
380 rooted, herbaceous vegetation cover replaces the current, more deeply rooted vegetation, either

381 as a consequence of shifting climate or land cover change. These transitions result in a nearly
382 three-fold decrease in our two relatively deep rooting depth metrics (D95 and D99) and a two-
383 fold decrease in D50 by the year 2100, suggesting that roots across Earth's subsurface will be
384 subject to extensive additional anthropogenic changes in the future and that the deepest roots
385 appear especially vulnerable to loss.

386

387 The global patterns we observed are strongly driven by trends in boreal and tundra regions,
388 where mapped scenarios suggest patterns of both root shallowing and deepening (Figs. 2, 4, S5,
389 and S6), and thus uncertainty about temporal dynamics of roots. While some studies hint that
390 roots may deepen as soils currently designated as permafrost thaw (Harsch et al., 2009; Sistla et
391 al., 2013; Malhotra et al., 2020; Wang et al., 2020), others suggest that long term changes in
392 snowpack will produce extremes in soil freeze/thaw cycles that will reduce vegetation survival
393 and rooting depth (Groffman et al., 2001; Blume-Werry et al., 2016). Most of our scenarios
394 suggest deepening of D99 and D95 in northern regions over time, lending support to findings of
395 deepening roots as permafrost thaws (Figs. 3 and 4) . However, contemporary D50 maps
396 demonstrate shallowing relative to potential vegetation in these same regions (Fig. S6), implying
397 that roots in boreal and tundra regions may be experiencing a more general change in the
398 curvature of rooting depth distributions instead of consistently deepening over time. These
399 observations support findings of altered root distributions where permafrost experiences altered
400 seasonal cycles, such as longer growing seasons (Blume-Werry et al. 2019). Data describing
401 rooting depths in these regions are more limited than in many other ecoregions (Iversen et al.,
402 2021; NEON 2021), resulting in less certainty about future rooting depths in areas currently
403 underlain by permafrost, and likely leading to the varied findings in our maps.

404

405 In maps of D50, additional regions also suggest that rooting depth distributions are undergoing a
406 general change in curvature as a response to anthropogenic change. Shallowing D50 values are
407 evident across potential, contemporary, and future scenarios (Figs. 3, 4, S5 and S6), and these
408 D50 metrics appear to become shallower to a greater extent between contemporary and future
409 (i.e., 2100) scenarios compared to the D50 changes that appear to have taken place already. This
410 finding suggests that anthropogenically-induced changes in the root abundances of surficial soil
411 horizons within the coming decades will likely exceed those of the past several millennia.

412 Shallowing D50 values occur alongside both shallowing and deepening of D99 and D95 values
413 in different regions of the globe, hinting of a trend of reshaped root distributions. Recently
414 collected data from the FRED and NEON databases make this change in curvature more
415 apparent than some of the individual datasets on which they build (Canadell et al., 1996; Zeng,
416 2001; Schenk and Jackson, 2005), highlighting the importance of continuing to characterize the
417 distribution of roots across the globe for understanding both the depths to which roots proliferate,
418 and the shape of their depth distributions. These most recent advances in FRED and NEON D50
419 data emphasize that even relatively shallow soil horizons (*i.e.*, those expressed by D50), where
420 both natural and agricultural species root, will undergo redistribution in the coming decades,
421 with roots shifting the curvature of their distributions in response to regional changes in land use
422 and climate.

423

424 There are myriad feasible consequences of altered rooting depth distributions for biogeochemical
425 and hydrological fluxes that prompt intriguing hypotheses. For example, roots beneath the zone
426 of maximum rooting density are attributed to developing the soils that mantle Earth's surface, so
427 much so that they are referred to as the planet's biotic weathering front, where life — roots and
428 microbes — promotes the dissolution of bedrock (Richter & Markewitz, 1995; Berner et al.,
429 2003; Brantley et al., 2012; Pawlik, 2013; Dontsova et al., 2020). Results from the current study
430 suggest that these biotic weathering forces in many temperate and tropical regions do not reach
431 as deeply into the regolith as they did prior to human influence (Figure 3), prompting the
432 hypothesis that the intensity of biotic processes responsible for soil formation at the bottom of
433 the soil profile have declined in the Anthropocene. Further, a smaller volume of soil explored by
434 rooting systems of some regions prompts the hypothesis that soil water storage capacity, nutrient
435 replenishment, and solute losses from freshly weathered material have similarly declined
436 (Swank, 1986; Nepstad et al., 1994; Berner, 1998). In contrast, in regions where root deepening
437 is occurring, we might expect increases in the influences of biotic weathering deep in the soil
438 profile.

439

440 Our findings serve as a useful starting point for formulating and probing these hypotheses.
441 Although this study makes a first attempt at measuring the extent of anthropogenically-induced
442 changes in rooting systems at a global scale, it also points to key knowledge gaps. The

443 uncertainty embedded in the projections reported here highlights the substantial need for better
444 quantification of rooting distributions in diverse biomes, particularly for deep roots, and how we
445 quantify their future dynamics. One challenge to global root quantification is the lack of
446 correspondence between potential, contemporary and future land cover classifications. These
447 incongruencies sometimes result in estimated changes in regionally-specific rooting depths that
448 contrast with current knowledge about anticipated vegetation transitions. In the current study,
449 place-based literature provided invaluable constraints on rooting depths for many ecosystems,
450 but rooting depths in many regions of Asia, Australia, and Africa remain understudied. A lack of
451 data describing contemporary rooting depth distributions in northern regions and estimates of
452 vegetative cover and associated rooting depths in the future also emerged as important
453 knowledge gaps (see especially Figure 1c). Additionally, there is a great deal of uncertainty in
454 estimates of the deepest roots worldwide (Shenk & Jackson, 2002). Indeed, many of the deepest
455 roots have been observed incidentally, suggesting that we have not yet sampled roots to their
456 fullest extent (Fan et al., 2017).

457

458 We suggest that CZ research combining empirical and modeling approaches could help focus
459 future research efforts on these critical gaps. First, empirical studies clarifying the ways in which
460 global rooting distributions are changing could help with the development of decadal- to
461 centennial-scale responses of extant ecosystems to climate change. Specifically, the leveraging
462 of on-going climate experiments (e.g., Caplan et al., 2019), naturally existing climatic gradients
463 (e.g., Ziegler et al., 2017), and chronosequences (e.g., Billings et al., 2018) could demonstrate
464 how rooting depths respond to global changes to temperature and precipitation, as well as reveal
465 quantitative relationships between rooting depth distributions and their impacts on soil formation
466 processes, especially at depth. Focusing these studies in regions with relatively less research will
467 improve our understanding of root-induced processes at the global scale.

468

469 Additionally, empirical and modeling studies examining the biogeochemical consequences of
470 rooting depth change are critical. More extensive work either directly measuring subsurface
471 biogeochemical fluxes as they respond to changes in rooting depth distributions, or modeling of
472 biogeochemical processes that project such fluxes, will be invaluable for generating input
473 parameters representing subsurface biogeochemical fluxes in ESMs. Because terrestrial

474 vegetation exerts a fundamental global control on land-atmosphere exchanges of water, energy,
475 C, and other elements, improved representation of rooting distributions in global land models
476 such as the Community Land Model (Lawrence et al., 2019) is of critical importance. This is
477 particularly true as more sophisticated aboveground and belowground vegetation and
478 biogeochemical processes are incorporated into these models (e.g., Tang et al., 2013; Fisher et
479 al., 2017; Kennedy et al., 2019). With improved fidelity to biophysical and biogeochemical
480 processes comes the corresponding opportunity to explore the potential consequences of changes
481 in global rooting depths on land-atmosphere exchanges of water, energy, and C, and the large-
482 scale ramifications that changes in rooting depths have for climate. Well-designed numerical
483 experiments could elucidate the relative impacts of exogenous (e.g., agricultural conversion,
484 woody encroachment) versus endogenous (e.g., water and nutrient limitation) drivers of changes
485 in rooting depths on terrestrial cycling of water, energy, and C. These modeling efforts can
486 feedback into empirical studies by illuminating regions where rooting depth knowledge is not
487 sufficient and by pointing toward parameters requiring more explicit definition to improve future
488 predictions. Such integrative studies would strengthen the nascent interactions between ESM and
489 CZ communities to address pressing questions about global change that cannot be solved without
490 substantial input from both disciplines (National Academy of Sciences, Engineering and
491 Medicine, 2020). The improved representation of changing rooting depth distributions can link
492 these research communities, representing a critical collaboration for understanding current and
493 future functioning of Earth's CZ and climate.

494 **5 Conclusion**

495 Losses of relatively deep roots suggest an overlooked and subtle mechanism by which humans
496 alter soil and ecosystem development. It is well established that humans accelerate losses of
497 surface soil via erosion, which can result in a thinning of Earth's skin of soil (Wilkinson and
498 McElroy, 2007). In contrast, altered rooting depths deep in soil profiles and associated shifts in
499 rooted volume due to anthropogenic land use and climate change suggest a means by which
500 human actions may govern soil thickness near the bottom of soil profiles. These shifts in rooting
501 distributions support the idea that signals of the Anthropocene penetrate deeply into the
502 subsurface even in naturally-occurring elemental cycles (Billings et al., 2018). Indications of
503 widespread human transformation of land cover across millennia (Edgeworth et al., 2015) imply

504 that reductions in deep root abundances have been underway in multiple regions for a similar
505 length of time. Though improving process representation in land models continues apace (Fisher
506 and Koven, 2020), the representation of rooting depth distributions remains largely a static
507 function of only PFT (cf. Drewniak, 2019). We present an opportunity to advance a dynamic
508 representation of roots in land models by better constraining how rooting depth distributions vary
509 with global change, as well as by identifying specific ecological processes particularly suited to
510 better quantifying the dynamics of rooting, both past and future (e.g., regions of woody
511 encroachment). Co-designed modeling, field and lab studies are needed to help clarify the
512 consequences of rooting depth changes for contemporary and future CZ development. Such
513 studies can elucidate the ways in which surficial anthropogenic activities radiate deep within
514 Earth's subsurface, altering the developmental pace and character of Earth's CZ.

515 **Acknowledgments**

516 We thank Drs. Jorge Soberón, A. Townsend Peterson, Daniel Richter and Pauly Cartwright for
517 offering helpful insights. We extend appreciation to Dr. Dan Markewitz for sharing his thoughts
518 about root extension into the subsoil, and to multiple anonymous reviewers for their comments.
519 Funding for this work was provided by NSF 1331846 and NSF 1841614. This material is also
520 based upon work supported by the National Science Foundation under Award No. OIA-1656006
521 and matching support from the State of Kansas through the Kansas Board of Regents.

522 **Data Availability and Code Availability**

523 The original GLC2000 dataset modified for this analysis can be accessed at
524 <https://forobs.jrc.ec.europa.eu/products/glc2000/products.php>. The unmodified potential
525 vegetation data can be found at https://daac.ornl.gov/cgi-bin/dsviewer.pl?ds_id=961. All future
526 land use projections can be accessed through the Landuse Harmonization data portal at
527 <http://luh.umd.edu/data.shtml>. Rasters modified as described in Methods for contemporary and
528 potential land cover, along with root depth assignment .csv files and code are available on

529 Zenodo (<https://doi.org/10.5281/zenodo.6522673>).

530

531 **Author Contributions**

532 SAB and EMH conceived of the idea with input from PLS. Analyses were developed and
 533 implemented by EMH and SAB. The manuscript was written by EMH and SAB with input from
 534 PLS, ANF and DH.

535 **References**

- 536 Andrade, E., Rosa, G. Q., Almeida, A. M., Silva, A. G. R. D., & Sena, M. G. T.
 537 (2020). Rainfall regime on fine root growth in a seasonally dry tropical forest. *Revista*
 538 *Caatinga*, *33*, 458-469.
- 539 Austin, J.J.C., Perry, A., Richter, D. D. & Schroeder, P. A. (2018). Modifications of 2:1 clay
 540 minerals in a kaolinite-dominated Ultisol under changing landuse regimes. *Clays and*
 541 *Clay Minerals*, *66*, 61-73. doi: 10.1346/CCMN.2017.064085
- 542
- 543 Bartolome, E. & Belward, A.S. (2005). GLC2000: A new approach to global land cover
 544 mapping from Earth observation data. *International Journal of Remote Sensing*, *26*,
 545 1959-1977. doi: 10.1080/01431160412331291297
- 546
- 547 Berner, R. A. (1998). The carbon cycle and carbon dioxide over Phanerozoic time: the role of
 548 land plants. *Philosophical Transactions of the Royal Society of London. Series B:*
 549 *Biological Sciences*, *353*, 75-82.
- 550 Berner, E. K., Berner, R. A., & Moulton, K. L. (2003). Plants and mineral weathering: present
 551 and past. *TrGeo*, *5*, 605. doi: 10.1098/rstb.1998.0192
- 552 Billings, S.A., Hirmas, D., Sullivan, P. L., Lehmeier, C. A., Bagchi, S., Min, K., Brecheisen, Z.,
 553 Hauser, E., Stair, R., Flournoy, R. & Richter, D.D. (2018). Loss of deep roots limits
 554 agents of soil development that are only partially restored by decades of forest
 555 regeneration. *Elementa Science of the Anthropocene*, *6*, 34.
 556 [doi:10.1525/elementa.287](https://doi.org/10.1525/elementa.287)
- 557 Billings, W. D., Peterson, K. M., Shaver, G. R., & Trent, A. W. (1977). Root growth, respiration,
 558 and carbon dioxide evolution in an arctic tundra soil. *Arctic and Alpine Research*, *9*, 129-
 559 137.
- 560 Boike, J., Juszak, I., Lange, S., Chadburn, S., Burke, E., Paul Overduin, P., ... & Gouttevin, I.
 561 (2018). A 20-year record (1998–2017) of permafrost, active layer and meteorological
 562 conditions at a high Arctic permafrost research site
 563 (Bayelva, Spitsbergen). *Earth System Science Data*, *10*, 355-390. doi: 10.5194/essd-10-
 564 355-2018
- 565

- 566 Blume-Werry, G., Kreyling, J., Laudon, H., & Milbau, A. (2016). Short-term climate change
 567 manipulation effects do not scale up to long-term legacies: Effects of an absent snow
 568 cover on boreal forest plants. *Journal of Ecology*, 104, 1638-1648.
 569
- 570 Blume-Werry, G., Milbau, A., Teuber, L. M., Johansson, M., & Dorrepaal, E. (2019). Dwelling
 571 in the deep—strongly increased root growth and rooting depth enhance plant interactions
 572 with thawing permafrost soil. *New Phytologist*, 223, 1328-1339.
 573
- 574 Brandt, J.P., Flannigan, M.D., Maynard, D.G., Thompson, I.D. & Volney, W.J.A. (2013). An
 575 introduction to Canada's boreal zone: ecosystem processes, health, sustainability and
 576 environmental issues. *Environmental Reviews*, 21. doi:10. 1139/er-2013-0040..
 577
- 578 Brantley, S. L., Eissenstat, D. M., Marshall, J. A., Godsey, S. E., Balogh-Brunstad, Z., Karwan,
 579 D. L., Papuga, S. A., Roering, J., Dawson, T. E., Evaristo, J., Chadwick, O.,
 580 McDonnell, J. J., & Weathers, K. C. (2017). Reviews and syntheses: On the roles trees
 581 play in building and plumbing the Critical Zone. *Biogeosciences*, 14, 5115-5142.
 582 doi: [10.5194/bg-14-5115-2017](https://doi.org/10.5194/bg-14-5115-2017)
 583
- 584 Brantley, S. L., Lebedeva, M., & Hausrath, E. M. (2012). A geobiological view of weathering
 585 and erosion. *Fundamentals of Geobiology*, 205-227. doi: 10.1002/9781118280874.ch12
 586
- 587 Canadell, J., Jackson, R. B., Ehleringer, J. B., Mooney, H. A., Sala, O. E. & Schulze E-D.
 588 (1996). Maximum rooting depth of vegetation types at the global scale. *Oecologia*, 108,
 589 583-595. doi: 10.1007/BF00329030
 590
- 591 Caplan, J.S., Gimenez, D., Hirmas, D.R., Brunsell, N.A., Blair, J.M. & Knapp, A.K. (2019).
 592 Decadal-scale shifts in soil hydraulic properties as induced by altered precipitation. *Sci*
 593 *Adv.* 5 :eaau6635. doi:10.1126/sciadv.aau6635.
 594
- 595 Cramer, W., Bondeau, A., Woodward, I., Prentice, I., Betts, R., Brovkin, V., Cox, P., Fisher, V.,
 596 Foley, J., Friend, A., Kucharik, C., Lomas, M., Ramankutty, N., Sitch, S., Smith, B.,
 597 White, A. & Young-Molling, C.(2001). Global response of terrestrial ecosystem structure
 598 and function to CO₂ and climate change: results from six dynamic global vegetation
 599 models. *Global Change Biology*, 7, 357-373. doi:10.1046/j.13652486.2001.00383.x
 600
- 601 Day, S. D., Wiseman, P. E., Dickinson, S. B., & Harris, J. R. (2010). Contemporary concepts of
 602 root system architecture of urban trees. *Arboriculture & Urban Forestry*, 36, 149-159.
 603
- 604 Devine, A.P., McDonald, R.A., Quaiife, T. & Maclean, I.M.D. (2017). Determinants of woody
 605 Encroachment and cover in African savannas. *Oecologia*, 183, 939-951.
 606
- 607 Dontsova, K., Balogh-Brunstad, Z. & Chorover, J. (2020). Plants as Drivers of Rock Weathering.
 608 In *Biogeochemical Cycles* (eds K. Dontsova, Z. Balogh-Brunstad and G. Le Roux).
 609 doi:10.1002/9781119413332.ch2

- 610 Drewniak, B. A. (2019). Simulating Dynamic Roots in the Energy Exascale Earth System Land
611 Model. *Journal of Advances in Modeling Earth Systems*, *11*, 338–359. doi:
612 10.1029/2018MS001334
613
- 614 DuPont, S. T., Culman, S. W., Ferris, H., Buckley, D. H., & Glover, J. D. (2010). No-tillage
615 conversion of harvested perennial grassland to annual cropland reduces root biomass,
616 decreases active carbon stocks, and impacts soil biota. *Agriculture, ecosystems &*
617 *environment*, *137*, 25-32. doi: 10.1016/j.agee.2009.12.021
618
- 619 DuPont, S. T., Beniston, J., Glover, J. D., Hodson, A., Culman, S. W., Lal, R., & Ferris, H.
620 (2014). Root traits and soil properties in harvested perennial grassland, annual wheat, and
621 never-tilled annual wheat. *Plant and Soil*, *38*, 405-420.
622
- 623 Edgeworth, M., Richter, D. D., Waters, C., Haff, P., Neal, C. & Price, S. J. (2015). Diachronous
624 beginnings of the Anthropocene: The lower bounding surface of anthropogenic deposits.
625 *The Anthropocene Review*, *2*, 33-58. doi: 10.1177/2053019614565394
- 626 Ellis, E.C., Goldewijk, K. K. , Siebert, S., Lightman, D. & Ramankutty, N. (2010).
627 Anthropogenic transformation of the biomes, 1700 to 2000. *Global Ecology and*
628 *Biogeography*, *19*, 589-606. doi: 10.1111/j.1466-8238.2010.00540.x
- 629 Fan, Y., Miguez-Macho G., Jobbágy, E. G., Jackson, R. B. & Otero-Casal, C. (2017).
630 Hydrologic regulation of plant rooting depth. *Proceedings of the National. Academy of*
631 *Science USA*, *114*, 10572-10577. doi: 10.1073/pnas.1712381114
- 632 Fisher, R. A., & Koven, C. D. (2020). Perspectives on the Future of Land Surface Models and
633 the Challenges of Representing Complex Terrestrial Systems. *Journal of Advances in*
634 *Modeling Earth Systems*, *12*, 1–24. doi: [10.1029/2018MS001453](https://doi.org/10.1029/2018MS001453)
635
- 636 Fisher, R. A., Koven, C. D., Anderegg, W. R. L., Christoffersen, B. O., Dietze, M. C., Farrior, C.
637 E., Holm, J. A., Hurtt, G. C., Knox, R. G., Lawrence, P. J., Lichstein, J. W., Longo, M.,
638 Matheny, A. M., Medvigy, D., Muller-Landau, H. C., Powell, T. L., Serbin, S. P., Sato,
639 H., Shuman, J. K., ... Moorcroft, P. R. (2017). Vegetation demographics in Earth System
640 Models: A review of progress and priorities. *Global Change Biology*, *24*, 35–54. doi:
641 10.1111/gcb.13910
642
- 643 Groffman, P. M., Driscoll, C. T., Fahey, T. J., Hardy, J. P., Fitzhugh, R. D., & Tierney, G. L.
644 (2001). Colder soils in a warmer world: a snow manipulation study in a northern
645 hardwood forest ecosystem. *Biogeochemistry*, *56*, 135-150.
646
- 647 Gupta, A.K. (2004). Origin of agriculture and domestication of plants and animals linked to
648 early Holocene climate amelioration. *Current Science*, *87*, 54-59.
- 649 Harsch, M. A., Hulme, P. E., McGlone, M. S., & Duncan, R. P. (2009). Are treelines advancing?
650 A global meta-analysis of treeline response to climate warming. *Ecology Letters*, *12*,
651 1040-1049. doi: 10.1111/j.1461-0248.2009.01355.x
- 652 Hasenmueller, E.A., Gu, X., Weitzman, J. N., Adams, T. S., Stinchcomb, G. E., Eissenstat, D.
653 M., Drohan, P. J., Brantley, S. L., Kaye, J. P. (2017). Weathering of rock to regolith: The

- 654 activity of deep roots in bedrock fractures. *Geoderma*, 300, 11-31.
655 doi: 10.1016/j.geoderma.2017.03.020
- 656 Haxeltine, A., & Prentice, I. C. (1996). BIOME3: An equilibrium terrestrial biosphere model
657 based on ecophysiological constraints, resource availability, and competition among plant
658 functional types. *Global Biogeochemical Cycles*, 10, 693-709. doi: 10.1029/96GB02344
- 659 Hertel, D., Harteveld, M. A., & Leuschner, C. (2009). Conversion of a tropical forest into
660 agroforest alters the fine root-related carbon flux to the soil. *Soil Biology and*
661 *Biochemistry*, 41, 481-490. doi: 10.1016/j.soilbio.2008.11.020
- 662 Hijmans, R. J., van Etten, J., Sumner, M., Cheng, J., Baston, D., Bevan, A., et al. (2019).
663 “Geographic Data Analysis and Modeling,” (CRAN, v. 3.0-7, 2019; [https://cran.r-](https://cran.r-project.org/web/packages/raster/raster.pdf)
664 [project.org/web/packages/raster/raster.pdf](https://cran.r-project.org/web/packages/raster/raster.pdf)).
- 665 Hurtt, G. C., Chini, L. P., Frohling, S., Betts, R. A., Feddema, J., Fischer, G., ... & Jones, C. D.
666 (2011). Harmonization of land-use scenarios for the period 1500–2100: 600 years of
667 global gridded annual land-use transitions, wood harvest, and resulting secondary lands.
668 *Climatic Change*, 109, 117. doi: 10.1007/s10584-011-0153-2
- 669
- 670 Hurtt, G. C., Chini, L., Sahajpal, R., Frohling, S., Bodirsky, B. L., Calvin, K., Doelman, J. C.,
671 Fisk, J., Fujimori, S., Goldewijk, K. K., Hasegawa, T., Havlik, P., Heinemann, A.,
672 Humpenöder, F., Jungclaus, J., Kaplan, J., Kennedy, J., Kristzin, T., Lawrence, D.,
673 Lawrence, P., Ma, L., Mertz, O., Pongratz, J., Popp, A., Poulter, B., Riahi, K.,
674 Shevliakova, E., Stehfest, E., Thornton, P., Tubiello, F. N., van Vuuren, D. P., and
675 Zhang, X. (2020). Harmonization of Global Land-Use Change and Management for the
676 Period 850–2100 (LUH2) for CMIP6. *Geosci. Model Dev. Discuss.*, 13, 5425-5464.
677 <https://doi.org/10.5194/gmd-2019-360>.
- 678 Iversen, C.M. (2010). Digging deeper: Fine-root responses to rising atmospheric CO₂
679 concentration in forested ecosystems. *New Phytologist*, 186, 346-357.
680 doi: 10.1111/j.1469-8137.2009.03122.x
- 681 Iversen, C. M., McCormack, M. L., Powell, A. S., Blackwood, C. B., Freschet, G. T., Kattge, J.,
682 ... & van Bodegom, P. M. (2017). A global fine-root ecology database to address below-
683 ground challenges in plant ecology. *New Phytologist*, 215, 15-26.
684
- 685 Iversen, C.M., McCormack, M. L., Baer, J.K., Powell, A.S., Chen, W., Collins, C., ... &
686 Zadworny, M. (2021). Fine-Root Ecology Database (FRED): A global collection of root
687 trait data with coincident site, vegetation, edaphic, and climatic data, version 3. Oak
688 Ridge National Laboratory, TES SFA, U.S. Department of Energy, Oak Ridge,
689 Tennessee, U.S.A. Access on-line at: <https://doi.org/10.25581/ornlsfa.014/1459186>.
- 690 Jackson, R.B., Canadell, J., Ehleringer, J. R., Mooney, H. A., Sala, O.E. & Schulze, E. D. (1996).
691 A global analysis of root distributions for terrestrial biomes. *Oecologia*, 108, 389-411.
692 doi: 10.1007/BF00333714
- 693 Jaramillo, V. J., Ahedo-Hernández, R., & Kauffman, J. B. (2003). Root biomass and carbon in a
694 tropical evergreen forest of Mexico: changes with secondary succession and forest
695 conversion to pasture. *Journal of Tropical Ecology*, 19, 457-464. doi: 10.
696 1017/S0266467403003493

- 697
698 Jobbagy, E. G. & Jackson, R. B. (2001) The distribution of soil nutrients with depth: Global
699 patterns and the imprint of plants. *Biogeochemistry*, 53, 51-77.
700 doi: 10.1023/A:1010760720215
701
- 702 Jordan, T. Ashley G. M., Barton, M. D., Burges, S. J., Farley, K. A., Freeman, K. H., Jeanloz, R.,
703 Marshall, C. R., Orcutt, J.A., Richter, F.M. et al. (Eds.). (2001). *Basic research
704 opportunities in Earth Science*. Washington D.C.: National Academy Press.
705
- 706 Kennedy, D., Swenson, S., Oleson, K. W., Lawrence, D. M., Fisher, R., Lola da Costa, A. C., &
707 Gentine, P. (2019). Implementing Plant Hydraulics in the Community Land Model,
708 Version 5. *Journal of Advances in Modeling Earth Systems*, 11, 485–513. doi:
709 [10.1029/2018MS001500](https://doi.org/10.1029/2018MS001500)
710
- 711 Keuper, F., Wild, B., Kummu, M., Beer, C., Blume-Werry, G., Fontaine, S., ... & Dorrepaal, E.
712 (2020). Carbon loss from northern circumpolar permafrost soils amplified by rhizosphere
713 priming. *Nature Geoscience*, 13, 560-565.
714
- 715 Kleidon, A. (2003). Global datasets of rooting zone depth inferred from inverse methods.
716 *Journal of Climate*, 17, 2741-2722. doi: 10.1175/1520-
717 0442(2004)017<2714:GDORZD>2.0.CO;2
718
- 719 Kleidon, A. & Heimann M. (1998). A method of determining rooting depth from a terrestrial
720 biosphere model and its impacts on the global water and carbon cycle. *Global Change
721 Biology*, 4, 275-286. doi: 10.1046/j.1365-2486.1998.00152.x
722
- 723 Krasowski, M. J., Lavigne, M. B., Szuter, M. A., Olesinski, J., Kershaw, J. A., & McGarrigle, E.
724 (2018). Age-related changes in survival and turnover rates of balsam fir (*Abies balsamea*
725 (L.) Mill.) fine roots. *Tree physiology*, 38, 865-876.
726
- 727 Lal, R. (2001). Potential of desertification control to sequester carbon and mitigate the
728 greenhouse effect. *Climatic change*, 51, 35-72.
729
- 730 Lander, J.P. (2013). *R for everyone: Advanced analytics and graphics*. Addison-Wesley, Boston,
731 MA.
732
- 733 Lawrence, D. M., Fisher, R. A., Koven, C. D., Oleson, K. W., Swenson, S. C., Bonan, G.,
734 Collier, N., Ghimire, B., Kampenhout, L., Kennedy, D., Kluzek, E., Lawrence, P. J., Li,
735 F., Li, H., Lombardozzi, D., Riley, W. J., Sacks, W. J., Shi, M., Vertenstein, M., ... Zeng,
736 X. (2019). The Community Land Model Version 5: Description of New Features,
737 Benchmarking, and Impact of Forcing Uncertainty. *Journal of Advances in Modeling
738 Earth Systems*, 11, 4245–4287. doi: 10.1029/2018MS001583

- 739 Lawrence, D. M., & Slater, A. G. (2005). A projection of severe near-surface permafrost
740 degradation during the 21st century. *Geophysical Research Letters*, *32*, L24401.
741 doi:10.1029/2005GL025080.
- 742 Lindsey, P., & Bassuk, N. (1992). Redesigning the urban forest from the ground below: A new
743 approach to specifying adequate soil volumes for street trees. *Arboricultural Journal*, *16*,
744 25-39.
- 745 Lozanova, L., Zhiyanski, M., Vanguelova, E., Doncheva, S., Marinov, M. P., & Lazarova, S.
746 (2019). Dynamics and vertical distribution of roots in European Beech forests and
747 Douglas Fir plantations in Bulgaria. *Forests*, *10*, 1123.
- 748 Maeght, J. L., Rewald, B. & Pierret, A. (2013). How to study deep roots and why it matters.
749 *Frontiers in Plant Science*, *4*, 299. doi: 10.3389/fpls.2013.00299
- 750 Malhotra, A., Brice, D. J., Childs, J., Graham, J. D., Hobbie, E. A., Vander Stel, H.,
751 ...&Iversen, C. M. (2020). Peatland warming strongly increases fine-root growth.
752 *Proceedings of the National Academy of Sciences*, *117*, 17627-17634.
- 753 McCormack, M. L., Crisfield, E., Raczka, B., Schneckeburger, F., Eissenstat, D. M., &
754 Smithwick, E. A. (2015). Sensitivity of four ecological models to adjustments in fine root
755 turnover rate. *Ecological modelling*, *297*, 107-117.
756
- 757 McCormack, M. L., Guo, D., Iversen, C. M., Chen, W., Eissenstat, D. M., Fernandez, C. W., ...
758 & Reich, P. B. (2017). Building a better foundation: Improving root-trait measurements
759 to understand and model plant and ecosystem processes. *New Phytologist*, *215*, 27-37.
760
- 761 Montagnoli, A., Terzaghi, M., Giussani, B., Scippa, G. S., & Chiatante, D. (2018). An integrated
762 method for high-resolution definition of new diameter-based fine root sub-classes of
763 *Fagus sylvatica* L. *Annals of forest science*, *75*, 1-13.
764
- 765 National Academy of Sciences, Engineering and Medicine. (2020). *A Vision for NSF Earth*
766 *Sciences 2020-2030: Earth in Time*. Washington, DC: The National Academies Press.
767 <https://doi.org/10.17226/25761>.
768
- 769 NEON (National Ecological Observatory Network). Root biomass and chemistry, Megapit,
770 RELEASE-2021 (DP1.10066.001). <https://doi.org/10.48443/s6k6-8h54>. Dataset accessed
771 from <https://data.neonscience.org> on November 22, 2021
772
- 773 Nepstad, D.C., Carvalho, C. R. d., Davidson, E. A., Jipp, P. H., Lefebvre, P. A., Negreiros, G.
774 H., da Silva, E. D., Stone, T. A., Trumbore, S. E. & Vieira, S. (1994). The role of deep
775 roots in the hydrological and carbon cycles of Amazonian forests. *Nature*, *372*, 666-669.
776 doi: 10.1038/372666a0
- 777 Nippert, J.B. & Knapp, A.K. (2007). Linking water uptake with rooting patterns in grassland
778 species. *Oecologia*, *153*, 261-272. doi: 10.1007/s00442-007-0745-8
- 779
- 780 Pawlik, L. (2013). The role of trees in the geomorphic system of forested hillslopes—A review.

- 781 *Earth-Science Reviews*, 126, 250-265. doi: 10.1016/j.earscirev.2013.08.007
782
- 783 Pierret, A., Maeght, J. L., Clement, C., Montoroi, J. P., Hartman, C., & Gonkhamdee, S. (2016).
784 Understanding deep roots and their functions in ecosystems: An advocacy for more
785 unconventional research. *Annals of Botany*, 118, 621-625.
786 <https://doi.org/10.1093/aob/mcw130>
- 787 Price, D.T., Alfaro, R.I., Brown, K.J., Flannigan, M.D., Fleming, R.A., Hogg, E.H., ... & Venier,
788 L.A. (2013). Anticipating the consequences of climate change for Canada's boreal forest
789 ecosystems. *Environmental Reviews*, 21, 322-326.
- 790 Ramankutty, N. & Foley, J.A. (1999). Estimating historical changes in global land cover:
791 Croplands from 1700 to 1992. *Global Biogeochemical Cycles*, 13, 997-1027.
792 [doi: 10.1029/1999GB900046](https://doi.org/10.1029/1999GB900046)
793
- 794 Richter, D. D. & Markewitz, D. (1995). How deep is soil? *BioScience*, 45, 600-609. doi:
795 10.2307/1312764
796
- 797 Riahi, K., Van Vuuren, D. P., Kriegler, E., Edmonds, J., O'Neill, B. C., Fujimori, S., ... & Lutz,
798 W. (2017). The shared socioeconomic pathways and their energy, land use, and
799 greenhouse gas emissions implications: an overview. *Global Environmental Change*, 42,
800 153-168.
- 801 RStudio Team. (2017). "RStudio: Integrated development for R," (RStudio Inc, Boston,
802 <http://www.rstudio.com/>).
803
804
- 805 Schenk, J. H. (2007). The shallowest possible water extraction profile: A null model for global
806 root distributions. *Vadose Zone Journal*, 7, 1119-1124.
807 doi: 10.2136/vzj2007.0119
808
- 809 Schenk, H. J. & Jackson, R.B. (2002a). The global biogeography of roots. *Ecological*
810 *Monographs*, 72, 311-328.
811
- 812 Schenk, H. J. & Jackson R.B. (2002b). Rooting depths, lateral root spreads, and
813 belowground/aboveground allometries of plants in water limited ecosystems. *Journal of*
814 *Ecology*, 90, 480-494.
815
- 816 Schenk, H. J. & Jackson, R.B. (2003). Global Distribution of Root Profiles in Terrestrial
817 Ecosystems. Data set with documentation. Available from the Oak Ridge National

- 818 Laboratory Distributed Active Archive Center, Oak Ridge, Tennessee, U.S.A. On-line at
819 <http://www.daac.ornl.gov>.
820
- 821 Schenk, H. J., & Jackson, R.B.. (2005). Mapping the global distribution of deep roots in
822 relation to climate and soil characteristics. *Geoderma*, 126, 129-140.
823
- 824 Schenk, H.J., & Jackson, R.B. 2009. ISLSCP II Ecosystem Rooting Depths. In Hall, Forrest G.,
825 G. Collatz, B. Meeson, S. Los, E. Brown de Colstoun, and D. Landis (eds.). ISLSCP
826 Initiative II Collection. Data set. Available on-line [<http://daac.ornl.gov/>] from Oak Ridge
827 National Laboratory Distributed Active Archive Center, Oak Ridge, Tennessee, U.S.A.
828 doi:10.3334/ORNLDAAAC/929
829
- 830 Sistla, S. A., Moore, J. C., Simpson, R. T., Gough, L., Shaver, G. R., & Schimel, J. P.
831 (2013). Long-term warming restructures Arctic tundra without changing net soil
832 carbon storage. *Nature*, 497, 615-618.
- 833 Stevens, N., Lehmann, C. E. R., Murphy, B. P. & Durigan, G. (2017). Savanna woody
834 encroachment is widespread across three continents. *Global Change Biology*, 23, 235-
835 244. doi: 10.1111/gcb.13409
836
- 837 Stone, E. L., & Kalisz, P. J. (1991). On the maximum extent of tree roots. *Forest ecology and*
838 *management*, 46, 59-102.
839
- 840 Sullivan, P. L., Billings, S. A., Hirmas, D., Li, L., Zhang, X., Ziegler, S., ... & Wen, H. (2022).
841 Embracing the dynamic nature of soil structure: A paradigm illuminating the role of life
842 in critical zones of the Anthropocene. *Earth-Science Reviews*, 225, 103873.
843
- 844 Swank, W. T. (1986). Biological control of solute losses from forest ecosystems (Vol. 85). John
845 Wiley & Sons, New York.
- 846 Tang, J. Y., Riley, W. J., Koven, C. D., & Subin, Z. M. (2013). CLM4-BeTR, a generic
847 biogeochemical transport and reaction module for CLM4: Model development,
848 evaluation, and application. *Geosci. Model Dev.*, 6, 127–140. doi: 10.5194/gmd-6-127-
849 2013
850
- 851 Wang, J. A., Sulla-Menashe, D., Woodcock, C. E., Sonnentag, O., Keeling, R. F., & Friedl, M.
852 A. (2020). Extensive land cover change across Arctic–Boreal Northwestern North
853 America from disturbance and climate forcing. *Global Change Biology*, 26, 807-822. doi:
854 [10.1111/gcb.14804](https://doi.org/10.1111/gcb.14804)
855
- 856 Whitford, W. G., & Duval, B. D. (2019). *Ecology of desert systems*. Academic Press.
857
- 858 Wilkinson, B. H., & McElroy, B. J. (2007). The impact of humans on continental erosion and
859 sedimentation. *Geological Society of America Bulletin*, 119, 140-156. doi:
860 10.1130/B25899.1

- 861
862 Zhang, T., Barry, R. G., Knowles, K., Heginbottom, J. A., & Brown, J. (2008). Statistics and
863 characteristics of permafrost and ground-ice distribution in the Northern Hemisphere.
864 *Polar Geography*, 31, 47-68. doi: 10.1080/10889370802175895
- 865
866 Zhang, Y., Niu, J., Yu, X., & Zhu, W. (2015). Effects of fine root length density and root
867 biomass on soil preferential flow in forest ecosystems. *Forest Systems*, 24, e012.
868 [doi: 10.5424/fs/2015241-06048](https://doi.org/10.5424/fs/2015241-06048)
- 869
870 Zhao, H. L., Zhao, X. Y., Zhou, R. L., Zhang, T. H., & Drake, S. (2005a). Desertification
871 processes due to heavy grazing in sandy rangeland, Inner Mongolia. *Journal of arid*
872 *environments*, 62, 309-319.
- 873
874 Zhao, M., Heinsch, F. A., Nemani, R. R., & Running, S. W. (2005b). Improvements of the
875 MODIS terrestrial gross and net primary production global data set. *Remote sensing of*
876 *Environment*, 95, 164-176. doi: 10.1016/j.rse.2004.12.011
- 877
878 Zeng, X. (2001). Global vegetation root distribution for land modeling. *American*
879 *Meteorological Society*, 2, 525-530. doi: 10.1175/1525-7
880 541(2001)002<0525:GVRDFL>2.0.CO;2
- 881
882 Ziegler, S.E., Benner, R., Billings, S.A., Edwards, K.A., Philben, M., Zhu, X. & Laganière, J.
883 (2017). Climate warming can accelerate carbon fluxes without changing soil carbon
884 stocks. *Frontiers in Earth Science*, 5, 2. doi:10.3389/feart.2017.00002
- 885